

Galactic chemical abundance distributions in a Λ CDM universe

Andreea S. Font¹, Kathryn V. Johnston¹, James S. Bullock² and
Brant Robertson³

¹Van Vleck Observatory, Wesleyan University Middletown, CT , 06459, USA

²Department of Physics & Astronomy, University of California, Irvine, CA 92687, USA

³Harvard-Smithsonian Center for Astrophysics, 60 Garden Street, Cambridge, MA 02138, USA

Abstract. Observations suggest systematic differences between chemical abundances of stars in satellite galaxies and those in the Milky Way halo. Specifically, for the same [Fe/H] values, stars in surviving satellite galaxies display significantly lower $[\alpha/\text{Fe}]$ ratios than stars in the stellar halo.

Here we investigate whether the observed differences can be explained in the framework of hierarchical structure formation. We model the chemical enrichment of a typical Milky Way galaxy in a Λ CDM Universe using, in combination, *i*) a semi-analytical code and numerical simulations that model the accretion and disruption of halo substructure and *ii*) a chemical evolution model that takes into account each satellite's star formation, metal enrichment and stellar feedback. Our results suggest that the observed chemical abundance patterns are a natural outcome in the process of hierarchical assembly of the Galaxy. We find that the stellar halo is built up from satellite galaxies accreted early on (more than 8–9 Gyr ago) and enriched in α -elements produced in Type II supernovae (average $[\alpha/\text{Fe}]$ values between 0.2–0.5). In contrast, satellites which survive today were typically accreted late (within the last 4–5 Gyr) and had at the time of accretion nearly solar $[\alpha/\text{Fe}]$ values as a result of the longer contribution of Type Ia supernovae.

1. Introduction

Recent observations have revealed interesting chemical abundance patterns in the Milky Way halo. Specifically, for the same [Fe/H] values, stars in neighboring satellite galaxies display $[\alpha/\text{Fe}]$ ratios significantly lower (by about 0.1–0.2 dex) than stars in the stellar halo (Shetrone *et al.* 2001, Shetrone *et al.* 2003, Venn *et al.* 2004). If Λ CDM is indeed a valid model for how galaxies form and evolve, then it has to explain the discrepancy in chemical abundances of different Galactic components. Following the chemical enrichment of the Galaxy in the full cosmological context is non trivial. In order to tackle this problem one has to have a model that incorporates a realistic merger history of a Milky Way-type galaxy, a detailed follow-up of the kinematics of substructure inside the galactic potential well and a chemical evolution model that includes an accurate treatment of stellar yields, the IMF and of winds from massive and intermediate mass stars. We present here a blending of two theoretical methods, one of constructing Milky Way-like stellar halos from accreting substructure (Bullock & Johnston 2004, Johnston & Bullock, in prep.) and the other of modeling the chemical evolution of individual satellite galaxies by taking into account both the inflow and outflow of matter (Robertson *et al.* 2005). The simulated galaxy has properties that match a series of observational constraints for the stellar halo (eg. total luminosity, gas content) and for its infalling

satellites as based on observations of Local Group dwarfs (eg. the stellar mass – circular velocity of dark halo relation, stellar mass - metallicity relation).

We describe below the results for a typical Milky Way halo. A detailed analysis of a larger sample of simulated halos will be presented in Johnston & Bullock (in prep.) and Font *et al.*(in prep.).

2. Results

Figure 1 shows the mass accretion history of one of our simulated stellar halos binned in time intervals of 0.2 Gyr. The top panel shows the accretion of the entire halo, and the bottom panel that of the inner $R < 20$ kpc region (here the radial distance R is centered on the position of the Sun, $R_{\odot} = 8.5$ kpc). The filled histograms represent the stellar material still gravitationally bound at present time ($t = 0$), whereas the empty histograms represent the entire accreted stellar mass. The figure shows that the stellar halo assembles early on. For example, $\sim 80\%$ of the inner halo (which is the counterpart of the “local halo” typically accessible in observations) is already in place by look-back time ~ 9 Gyr. The material still bound today (i.e. in surviving satellites) has been accreted more recently, generally within the past few Gyr. Not surprisingly, none of the surviving satellites are found in the inner region of the halo where tidal forces are strongest.

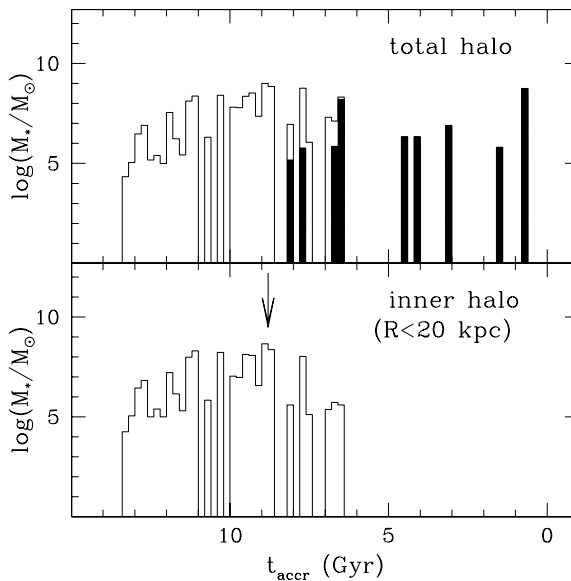


Figure 1. Mass accretion history of the simulated galaxy halo binned in time intervals of 0.2 Gyr. Filled histograms represent the stellar material still gravitationally bound at present time ($t = 0$), and empty histograms represent the entire accreted stellar mass. Top panel corresponds to the entire halo and bottom panel to the inner $R < 20$ kpc halo. The arrow in the bottom panel denotes the look-back time when $\sim 80\%$ of the inner halo has assembled.

These results are typical of all simulated halos and suggest that present day satellite galaxies of the Milky Way are likely to have been accreted recently. This implies that they also had more time available for sustaining star formation and hence further their chemical enrichment (our model assumes that most of star formation in satellite galaxies occurs prior to their accretion onto the main halo, after which their gas is stripped by ram pressure and thus star formation is shut off; the result is however largely independent

of this assumption, since the majority of satellites are fully disrupted within 1–2 orbits after accretion).

The chemical evolution of infalling substructure is investigated in Figure 2, which shows the $[\alpha/\text{Fe}]$ versus $[\text{Fe}/\text{H}]$ ratios of all baryonic satellites (values are averages weighted by the contribution of different stellar populations). Here $[\alpha/\text{Fe}]$ represents the average of $[\text{O}/\text{Fe}]$ and $[\text{Mg}/\text{Fe}]$ abundances. The left panel shows the abundance ratios plotted with different symbols function of their time of accretion. In the right panel we plot the same quantities, this time the different symbols denoting whether satellites are fully disrupted or still containing some bound material at $t = 0$. This figure shows that those satellites that enter the main potential well later tend to have higher $[\text{Fe}/\text{H}]$ and lower $[\alpha/\text{Fe}]$. This is because Fe content increases with time, with the most significant contribution coming from Type Ia supernova activity which sets on after first $\sim 1\text{--}2$ Gyr (Larson 1974). In contrast, α -elements being produced very early on in Type II supernovae have abundances that remain relatively constant in time (hence the decrease in $[\alpha/\text{Fe}]$ with time). Surviving satellites have the lowest $[\alpha/\text{Fe}]$ ratios and, on average, these values are 0.1–0.2 dex lower than that of the stellar halo (that is, of the material originating in the disrupted satellites) – in agreement with the observational results.

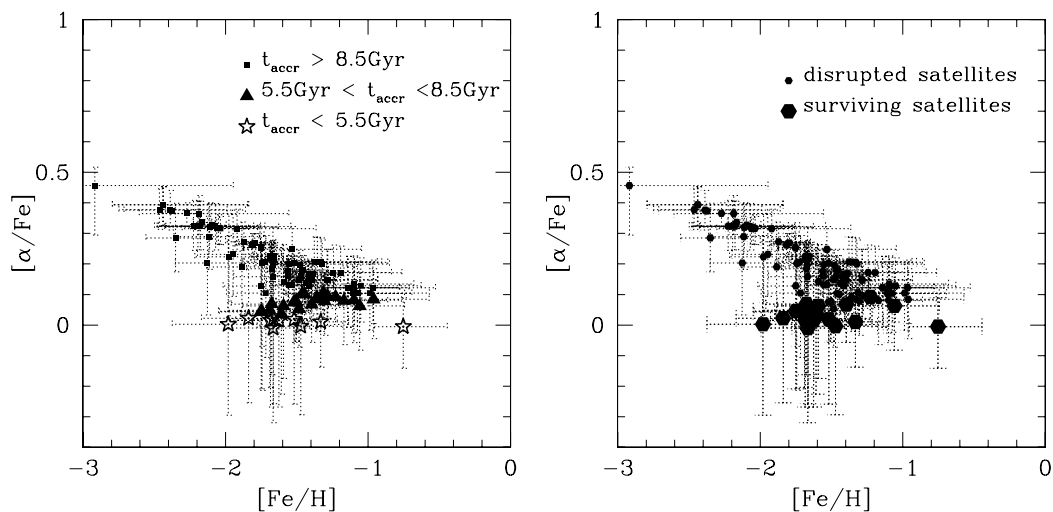


Figure 2. $[\alpha/\text{Fe}]$ versus $[\text{Fe}/\text{H}]$ for all baryonic satellites accreted onto the main halo of the Milky Way -type galaxy. *Left:* Satellites are plotted with different symbols function of their look-back time of accretion: squares denote satellites accreted at $t_{\text{accr}} > 8.5$ Gyr, triangles those accreted $5.5 < t_{\text{accr}} < 8.5$ Gyr, and stars with $t_{\text{accr}} < 5.5$ Gyr. *Right:* Small and large symbols denote whether satellites are fully disrupted or still containing some bound material at present time ($t = 0$), respectively. Errorbars in both panels represent 10% and 90% of the weighted average values.

3. Conclusions

We have shown that the observed differences between chemical abundances of surviving satellites and halo can be naturally understood in the framework of the Λ CDM model. Thus satellites surviving at present time were generally accreted late and had more time available for chemical enrichment (notably Fe enrichment by Type Ia supernovae). In contrast, satellites accreted early (which make up, by mass, most of the halo) were

typically more deficient in Fe than their later counterparts, hence had higher $[\alpha/\text{Fe}]$ values when accreted.

Acknowledgements

A.F and K.V.J's contributions were supported through NASA grant NAG5-9064 and NSF CAREER award AST-0133617.

References

- Bullock, J.S. & Johnston, K.V. 2004, in *Satellites and Tidal Streams*, ed. F. Prada, D. Martinez-Delgado & T. Mahoney (San Francisco: ASP)
- Larson, R.B. 1974, *MNRAS* 169, 229
- Robertson, B. , Bullock, J. S., Font, A.S., Johnston, K.V. & Hernquist, L. 2005, *ApJ* submitted
- Shetrone, M.D., Côté, P. & Sargent, W.L.W. 2001, *ApJ* 548, 592
- Shetrone, M.D., Venn, K.A., Tolstoy, E., Primas, F., Hill, V. & Kaufer, A. 2003, *AJ* 125, 684
- Venn, K.A., Irwin, M., Shetrone, M.D., Tout, C.A., Hill, V. & Tolstoy, E. 2004, *AJ* 128, 1177

Discussion

DEKEL: What is the origin of the difference in metallicity between the stellar halo and the surviving satellites? How does the initial satellite mass translate to the final difference? Aren't gradients within the initial satellites relevant?

FONT: In terms of the $[\text{Fe}/\text{H}]$ distribution, the stellar halo and surviving satellites look about the same. The difference arises in the $[\alpha/\text{Fe}]$ ratios: surviving satellites tend to have lower $[\alpha/\text{Fe}]$ values than the local stellar halo. Among the satellites which become disrupted at present time, those with high initial mass are expected to contribute the most to the make-up of the halo. However, the stellar halo has also a non-negligible contribution from the low-mass, early accreted satellites, which tend to have higher $[\alpha/\text{Fe}]$ ratios. These satellites make most of the difference in $[\alpha/\text{Fe}]$ patterns of the stellar halo. Initial metallicity gradients are important and they will be preserved in the halo.

